

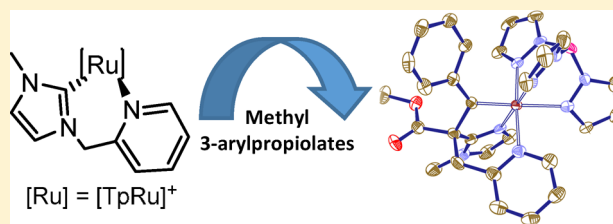
Functionalized N-Heterocyclic Carbene Nonspectator Ligands upon Internal Alkyne Activation Reactions

Francys E. Fernández, María del Carmen Puerta,* and Pedro Valerga*

Departamento de Ciencia de los Materiales e Ingeniería Metalúrgica y Química Inorgánica, Facultad de Ciencias, Universidad de Cádiz, 11510 Puerto Real, Cádiz, Spain

Supporting Information

ABSTRACT: When studying the activation of 3-arylpropiolates by $[\text{TpRu}(\text{picolyl-}^{\text{Me}}\text{I})\text{Cl}]/\text{NaBAR}_4^{\text{F}}$ ($\text{picolyl-}^{\text{Me}}\text{I}$ = 3-methyl-1-(2-picolyl)imidazol-2-ylidene (**1**); $\text{picolyl-}^{\text{Me}}\text{BI}$ = 3-methyl-1-(2-picolyl)benzimidazol-2-ylidene (**2**)) a migratory insertion of the NHC into a ruthenium–carbon bond and an unprecedented C–N bond activation of the chelating picolyl-NHC ligand take place to give the new ruthenium metallacycles $[\text{TpRu}(\kappa^3\text{-C}_3\text{-N,N'}\text{=C(Ph)-C(CH}_2\text{Py)(CO}_2\text{Me)}^{\text{Me}}\text{I})][\text{BAR}_4^{\text{F}}]$ **3a** and **4a** and $[\text{TpRu}(\kappa^3\text{-C}_3\text{-N,N'}\text{=C(4-CF}_3\text{Ph)-C(CH}_2\text{Py)(CO}_2\text{Me)}^{\text{Me}}\text{I})][\text{BAR}_4^{\text{F}}]$ **3b** and **4b**. X-ray crystal structures of **3a** and **3b** are reported, and a mechanistic pathway is proposed. In contrast, activation of internal alkynones by a mixture of $[\text{TpRu}(\text{picolyl-}^{\text{Me}}\text{I})\text{Cl}]$ complex (**1**) and $\text{NaBAR}_4^{\text{F}}$ led to isolation and characterization of the corresponding disubstituted vinylidene complexes. Also, structures of $[\text{TpRu}(\text{picolyl-}^{\text{Me}}\text{I})(=\text{CC(COR)(Ph)})][\text{BAR}_4^{\text{F}}]$ ($\text{R} = \text{Me}$ (**6a**); Ph (**6b**)) are reported.



INTRODUCTION

NHCs have been termed the most important ancillary ligands after cyclopentadienyls and extensively explored phosphines.¹ They have participated in the design of numerous improved catalysts, particularly because they are easily electronically and sterically tunable, and act as powerful σ donors. Until recently, they were referred as *noninterfering* supporting ligands;² however, their behavior is not always inert, being susceptible to reductive elimination,³ C–H and C–C bond activation reactions within the N-wingtip substituents,⁴ and rarely C–N bond activation.⁵ To overcome these potential issues, when attempting the synthesis of new homogeneous catalysts, functionalized NHCs with an additional donor group have appeared, giving the resulting NHC complexes more stability via an inflexible chelating coordination.⁶ Also, the potential hemilability of the additional donor group has attracted much attention. Our group has recently reported the synthesis of several ruthenium complexes bearing picolyl-NHC ligands, particularly $[\text{TpRu}(\text{picolyl-NHC})\text{Cl}]$ ⁷ and $[\text{Cp}^*\text{Ru}(\text{picolyl-NHC})(\text{CH}_3\text{CN})][\text{PF}_6]$.⁸

Although, Crabtree and co-workers described the possibility that C₂-bound imidazoles could exist in equilibrium with their N-bound tautomer,⁹ recently the first example of C- to N-bound tautomerism in which an NHC was directly involved was reported by Whittlesey and co-workers. The C-bound $[\text{RuHCl}(\text{PPh}_3)_2(\text{CO})(1\text{-isopropyl-4,5-dimethylimidazol-2-ylidene})]$ complex obtained after C–N activation of the NHC is subsequently converted into the N-1-bound product.¹⁰ In addition, Wang et al. reported the C- to N-bound tautomerization of an NHC induced by iridium.⁵ In both

cases aforementioned the C- to N-bound tautomerization is completed with a monodentate N-heterocyclic carbene.

In this work, we report that upon studying the reactivity of internal alkynpropiolates with $[\text{TpRu}(\text{picolyl-NHCs})]^+$ an unprecedented ruthenium-induced C–N bond activation and migratory insertion of an NHC into a ruthenium–carbon bond was completed, illustrating a new carbene degradation pathway even when a chelating NHC is used as ligand.

The activation process of 1-alkynes via formation of vinylidene metal complexes is well known.¹¹ However, conversion of internal alkynes to disubstituted vinylidenes via 1,2-migration ($\text{RC}\equiv\text{CR}' \rightarrow \text{:C}=\text{CRR}'$) is an undeveloped process.^{11a} Heteroatom-substituted internal alkynes as silane-alkynes,¹² tin alkynes,^{12d,13} 1-haloalkynes,^{12f,14} and mercaptoacetylene¹⁵ were reported to participate in vinylidene formation via the 1,2-R shift. Recently, migration of carbon substituents has emerged as a promising route for synthesis of new vinylidene complexes. Our group reported the rearrangement of internal alkynes and alkynones to the corresponding vinylidenes using TpRu fragments with mono- and bidentate phosphine ligands.¹⁶ Shaw et al. reported the use of $\text{CpRu}(\text{PPh}_3)_2\text{Cl}$ for η^1 -vinylidene formation from internal alkynones.¹⁷ Additionally, Ishii and co-workers reported direct formation of general disubstituted vinylidenes from aryl-, alkyl-, and carboxy-substituted internal alkynes using ruthenium and iron complexes and the reversibility of the process.¹⁸ Finally, during preparation of this work, Otsuka et al. reported a DFT study of internal alkyne to disubstituted vinylidene isomer-

Received: February 19, 2013

Published: May 10, 2013



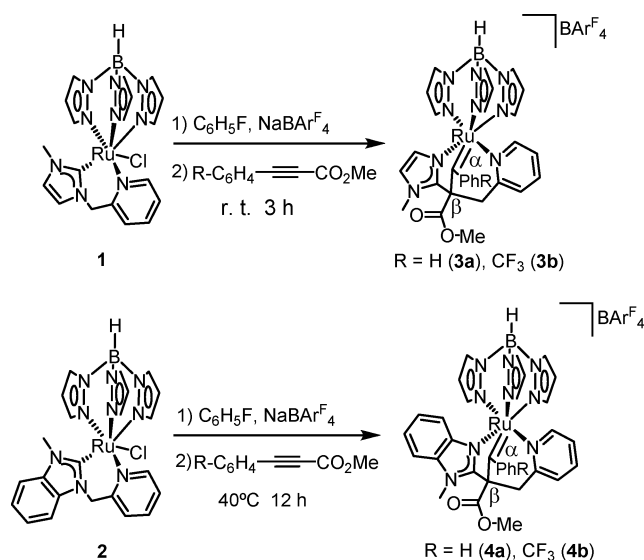
ization in $[\text{CpRu}(\text{PhC}\equiv\text{CC}_6\text{H}_4\text{R-p})(\text{dppe})]^+$ ($\text{R} = \text{OMe}$, CO_2Et , and Cl) demonstrating, using donor–acceptor analysis, that the aryl 1,2-shift is a nucleophilic reaction.¹⁹

The influence of transition-metal ligands in the activation of internal alkynes is key in assessing the scope of this transformation. This paper aims to provide new insights in the internal alkyne activation process using metal complexes bearing picolyl-NHCs and describe a new decomposition pathway for functionalized NHCs.

RESULTS AND DISCUSSION

Synthesis of C–N Activation and Migratory Insertion Products 3a, 3b, 4a, and 4b. Treatment of $[\text{TpRu}(\text{picolyl-}^{\text{Me}}\text{I})\text{Cl}]$ (**1**) and $[\text{TpRu}(\text{picolyl-}^{\text{Me}}\text{BI})\text{Cl}]$ (**2**) in the presence of $\text{NaBAR}_4^{\text{F}}$ ($\text{Ar}^{\text{F}} = 3,5\text{-bis(trifluoromethyl)phenyl}$) with a slight excess of internal alkyne $\text{RC}\equiv\text{CR}'$ ($\text{R}, \text{R}' = \text{Ph}$, COOMe ; $\text{R}, \text{R}' = 4\text{-CF}_3\text{C}_6\text{H}_4$, COOMe) resulted in unexpected formation of $[\text{TpRu}(\kappa^3\text{-C}_2\text{N,N}'\text{-C(R)-C(COOMe)(CH}_2\text{Py)}^{\text{(MeI)}})]\text{BAR}_4^{\text{F}}$ (**3a** and **3b**) and $[\text{TpRu}(\kappa^3\text{-C}_2\text{N,N}'\text{-C(R)-C(COOMe)(CH}_2\text{Py)}^{\text{(MeBI)}})]$ (**4a** and **4b**) as deep green or brown solids, respectively, in high yields of ca. 79–88% (Scheme 1).

Scheme 1



These compounds were air stable in the solid state and characterized by ^1H , $^{13}\text{C}\{^1\text{H}\}$ NMR, and IR spectroscopies as well as elemental analysis. Selected $^{13}\text{C}\{^1\text{H}\}$ NMR data of compounds **3a**, **3b**, **4a**, and **4b** are listed in Table 1. Carbon assignments were completed using ^1H – ^{13}C 2D NMR correlation experiments, HMQC, and HMBC. Noteworthy, the low-field resonances of the new ruthenium carbene carbons

Table 1. Selected $^{13}\text{C}\{^1\text{H}\}$ NMR Data for Compounds **3a**, **3b**, **4a**, and **4b**

| compd | $^{13}\text{C}\{^1\text{H}\}$ | | | |
|-----------|-------------------------------------|---------------------|-------------------------|------------------|
| | $\text{Ru}=\text{C}$ (C_α) | $\text{C}=\text{O}$ | $\text{C}_2\text{-NHC}$ | C_β |
| 3a | 329.3 | 171.4 | 147.7 | 75.7 |
| 3b | 326.9 | 170.7 | 147.1 | 76.3 |
| 4a | 331.1 | 172.1 | 155.7 | 78.0 |
| 4b | 329.2 | 171.5 | 154.1 | 78.7 |

(C_α) at 329.3, 326.9, 331.1, and 329.2, respectively, which in addition to the presence of new quaternary carbons, C_β , that appeared at 75.7, 76.3, 78.0, and 78.7, depending on the case, are the main spectroscopic characteristics of the migratory insertion and C–N activation completion. Also, the $\text{C}_2\text{-NHC}$ carbon resonances shifted their positions to higher fields in comparison to the starting products, **1** and **2**, as a direct consequence of the discoordination from the metal center. In none of the cases was there evidence for formation of the expected disubstituted vinylidene products. The need of higher temperature and longer reaction time to complete the transformation when **2** is used as starting complex may be justified by the different donor properties of the picolyl-benzimidazolylidene ligand when compared to its analog, **1**.⁷

Crystals of **3a** and **3b** suitable for X-ray diffraction studies were obtained after recrystallization from CH_2Cl_2 /petroleum ether (1/2). An ORTEP diagram of **3a** is displayed in Figure 1, along with selected interatomic distances and angles. Also, the X-ray crystal structure of **3b** is provided in the Supporting Information.

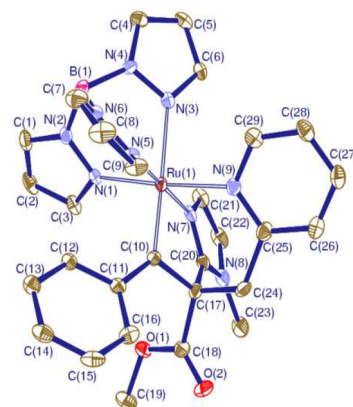


Figure 1. ORTEP view of the cation of $[\text{TpRu}(\kappa^3\text{-C}_2\text{N,N}'\text{-1-(1-phenyl-2-(1-methyl-1H-imidazol-2-yl)-3-pyridyl-prop-1-ylidene-2-carboxylic acid methyl ester)})]\text{BAR}_4^{\text{F}}$ (**3a**). Selected bond lengths (Angstroms) and angles (degrees): $\text{Ru(1)}\text{--}\text{C(10)}$ 1.873(6), $\text{Ru(1)}\text{--}\text{N(1)}$ 2.060(5), $\text{Ru(1)}\text{--}\text{N(3)}$ 2.196(5), $\text{Ru(1)}\text{--}\text{N(5)}$ 2.059(4), $\text{Ru(1)}\text{--}\text{N(7)}$ 2.059(4), $\text{Ru(1)}\text{--}\text{N(9)}$ 2.103(5), $\text{O(1)}\text{--}\text{C(18)}$ 1.329(8), $\text{O(1)}\text{--}\text{C(19)}$ 1.451(8), $\text{O(2)}\text{--}\text{C(18)}$ 1.202(8); $\text{N(1)}\text{--}\text{Ru(1)}\text{--}\text{N(9)}$ 175.3(2), $\text{N(3)}\text{--}\text{Ru(1)}\text{--}\text{C(10)}$ 177.3(2), $\text{N(5)}\text{--}\text{Ru(1)}\text{--}\text{N(7)}$ 177.8(2), $\text{O(1)}\text{--}\text{C(18)}\text{--}\text{O(2)}$ 124.9(6).

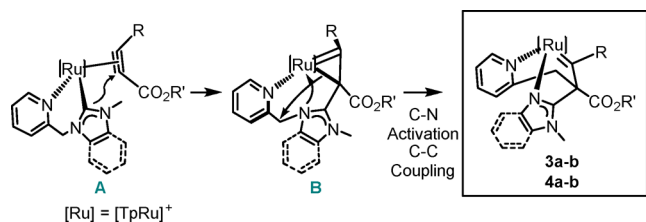
We are not aware of any previous reported structure of a $\text{Ru}=\text{CR}_2$ carbene moiety containing a quaternary C_β carbon atom. When the search is extended to any metal a few results appear, but in most of these complexes a tBu group is bonded to the carbenic carbon. The in-situ-formed ligand- $\kappa^3\text{C}_2\text{N,N}'$ coordinates facial opposite to the Tp ligand. The ruthenium coordination sphere is essentially octahedral with angles formed by cis donor atoms ranging from $\text{N(1)}\text{--}\text{Ru(1)}\text{--}\text{N(3)}$ $82.39(18)^\circ$ to $\text{N(3)}\text{--}\text{Ru(1)}\text{--}\text{N(7)}$ $96.07(18)^\circ$. As expected, the bond length enlarged in the opposite direction shows that the carbenic C exerts a more intense trans influence than the imidazolyl or pyridyl N donor atoms. On the other hand, the ester group adopts a trigonal planar geometry with a sp^2 -hybridized C(18) atom and an essentially localized $\text{C}=\text{O}$ double bond.

Several examples of the noninnocent behavior of NHC ligands have been documented. The work done by Kirchner

and co-workers studying insertion of NHCs in ruthenium–carbon double bonds as well as migration of acetylene in NHC complexes of ruthenium is particularly interesting.²⁰ Also, Fantasia et al. reported insertion of NHCs into a platinum olefin bond.²¹ However, only a few examples of tautomerization of C- to N-bound NHCs have been reported.^{5,10} Thus, this is a remarkable example of C- to N-bound tautomerism with a functionalized NHC which implies C–N bond activation. Considering the chelating nature of the picolyl-NHC ligand, the process is very rare.

On the basis of our experimental findings and previous experiences working with TpRu phosphine complexes, we proposed a reaction mechanism (Scheme 2) to explain this

Scheme 2. Proposed Mechanism for Formation of 3a, 3b, 4a, and 4b

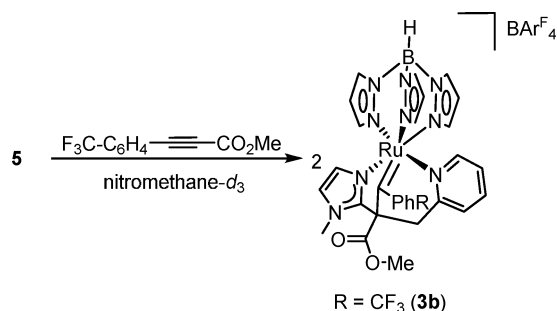


unusual reaction. The reasonable starting point is formation of a π -alkyne intermediate **A** upon completion of halide abstraction in the presence of the internal alkyne. **A** can undergo intramolecular attack of the coordinated NHC ligand at a nearby $\text{C}\equiv\text{C}$ bond, resulting in formation of a 1-metallacyclopropene complex **B**. In fact, Becker et al. suggested using DFT/B3LYP calculations for formation of a similar intermediate while studying the migratory insertion of acetylene in NHC complexes of ruthenium.²⁰ Rearrangement of **B** is expected considering the presence of two very restrained metallacycles with 7- and 3-membered rings. The most stable configuration is achieved after C–N activation of the picolyl-NHC ligand and the concerted C–C coupling reaction leading to **3a** and **3b** or **4a** and **4b** depending on the case. These structures contain 5- and 6-membered ring metallacycles.

In order to gain more insight into the reaction mechanism and possible intermediates, we conducted the NMR-scale reaction of the dinitrogen-bridged complex $[\{\text{TpRu}(\text{picolyl-}^{\text{Me}}\text{I})\}_2(\mu\text{-N}_2)][\text{BAr}^{\text{F}_4}]_2$, **5**,⁷ and a slight excess of $\text{CF}_3\text{C}_6\text{H}_4\text{C}\equiv\text{CCO}_2\text{Me}$ to give **3b** in nitromethane- d_3 (Scheme 3).

Quantitative kinetic measurements have been obtained by monitoring the evolution of the ^{19}F NMR signals of compound **3b** and methyl 3-(4-trifluoromethylphenyl)propiolate within an

Scheme 3



appropriate temperature range in nitromethane- d_3 . The singlet signal of the free internal alkyne (−64.2 ppm) decreases with time, while a new signal corresponding to **3b** that increases exponentially with time appears (−64.4 ppm). In all cases, the reaction obeys a first-order rate law. Thus, the rate constants at different temperatures have been obtained, and the corresponding Eyring plot (Figure 2) provides the activation parameters. Integral vs time plots and a table with the rate constants at each temperature can be found in the Supporting Information.

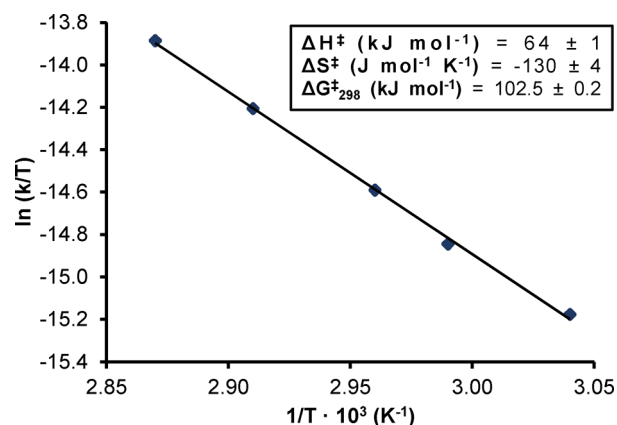
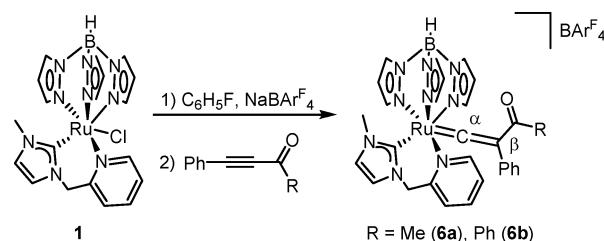


Figure 2. Eyring plot and activation parameters for reaction of **5** with $\text{CF}_3\text{C}_6\text{H}_4\text{C}\equiv\text{CCO}_2\text{Me}$ to yield **3b**.

We were not able to detect formation of any intermediate in the reaction mixture in terms of new peaks in the ^{19}F NMR spectrum to support our mechanism proposal. Thus, any intermediate must react quickly. The activation parameters point to an associative process. The negative activation entropy may be understood as a decrease of translational, rotational, and vibrational degrees of freedom on route to the transition state, suggesting a concerted C–N activation and C–C coupling reaction as proposed in Scheme 2 intermediate **B**. Also, the first-order kinetics implies that formation of intermediate **A** is not the rate-limiting step.

Synthesis and Characterization of Disubstituted Keto Vinylidene Complexes 6a and 6b. In order to assess the scope of the reaction of $[\text{TpRu}(\text{picolyl-NHC})]^+$ species toward internal alkynes, we tested the reactivity of **1** with a series of disubstituted alkynes $\text{RC}\equiv\text{CR}'$ ($\text{R}, \text{R}' = \text{Ph}, \text{COMe}; \text{Ph}, \text{COPh}; \text{Ph}, \text{Ph}; \text{Ph}, \text{Me}; \text{CO}_2\text{Et}, \text{CO}_2\text{Et}$). Activation of alkynes by **1** yielded the corresponding disubstituted vinylidenes. When a fluorobenzene solution of $[\text{TpRu}(\text{picolyl-}^{\text{Me}}\text{I})\text{Cl}]$ was allowed to react with $\text{PhC}\equiv\text{COR}$ ($\text{R} = \text{Me}; \text{Ph}$) in the presence of $\text{NaBAr}^{\text{F}_4}$ at room temperature (Scheme 4) disappearance of the initial yellow-red color and formation of a brown suspension was observed. In both cases,

Scheme 4



6a and **6b** were obtained in high yields of up to 82% as red crystals. Crystals were characterized by IR, NMR, and elemental analysis.

In contrast to our previous work regarding preparation of keto vinylidene complexes from $[\text{TpRu}(\kappa^2\text{-P,N-PyCH}_2\text{P}^i\text{Pr}_2)\text{-Cl}]$, the reaction did not require heating and no differences in reactivity were observed between the ketone substituents.¹⁶ In addition, we were not able to isolate the $\eta^1\text{-O-ketoalkyne}$ complexes, intermediates in the isomerization to secondary vinylidenes, as was the case when the starting products bore picolyl-phosphine ligands.¹⁶ Several attempts with shorter reaction times and lower reaction temperatures were completed, but in all cases, the crude reaction mixtures showed an uncharacterizable mixture of products that did not allow isolation of any intermediates of neither the π -alkyne nor the $\eta^1\text{-O-ketoalkyne}$ complexes. The summary of the main spectroscopic $^{13}\text{C}\{^1\text{H}\}$ NMR data for compounds **6a** and **6b** and the picolyl-phosphine analogues are shown in Table 2. The

Table 2. Selected $^{13}\text{C}\{^1\text{H}\}$ NMR Data for Compounds **6a** and **6b**, $[\text{TpRu}\{\text{=CC(OMe)Ph}\}(\kappa^2\text{-P,N-PyCH}_2\text{P}^i\text{Pr}_2)][\text{BAR}^{\text{F}}_4]^{16\text{a}}$ and $[\text{TpRu}\{\text{=CC(OPh)Ph}\}(\kappa^2\text{-P,N-PyCH}_2\text{P}^i\text{Pr}_2)][\text{BAR}^{\text{F}}_4]^{16\text{a}}$

| compd | $^{13}\text{C}\{^1\text{H}\}$ | | | |
|--|-------------------------------|-------------------------------|-------|-----------------------|
| | Ru=C (C_α) | RuC=C (C_β) | C=O | C_2 - NHC |
| 6a | 354.7 | 124.7 | 194.6 | 172.3 |
| 6b | 353.1 | 126.4 | 189.2 | 172.6 |
| $[\text{TpRu}\{\text{=CC(OMe)Ph}\}(\text{PyCH}_2\text{P}^i\text{Pr}_2)][\text{BAR}^{\text{F}}_4]^{16\text{a}}$ | 357.3 | 131.8 | 196.6 | |
| $[\text{TpRu}\{\text{=CC(OPh)Ph}\}(\text{PyCH}_2\text{P}^i\text{Pr}_2)][\text{BAR}^{\text{F}}_4]^{16\text{a}}$ | 356.5 | 131.5 | 189.9 | |

presence of the vinylidene carbon (C_α) is revealed by characteristic low-field resonances at 354.7 and 353.1 ppm for compounds **6a** and **6b**, respectively, fully comparable with those reported for the picolyl-phosphine analogues.¹⁶ Also, coordination of the NHC is confirmed by the characteristic carbene carbon (C_2) resonances at 172.3 and 172.6 ppm for **6a** and **6b**, respectively.

In addition to the spectroscopic data, compounds **6a** and **6b** have been characterized by X-ray diffraction analysis of monocrystals, grown from slow diffusion of petroleum ether into concentrated dichloromethane solutions of the complexes. Figure 3 shows an ORTEP view of the cation in **6a** along with selected bond lengths and angles. Also, the X-ray crystal structure of **6b** is provided in the Supporting Information.

The X-ray structure of $[\text{TpRu}\{\text{=C=C(OMe)Ph}\}(\kappa^2\text{-C,N-picolyl-MeI})]^+$ shows distorted octahedral coordination around the ruthenium center with three facial coordination sites occupied by the N atoms of the Tp ligand, two other positions by the C and N atoms of the picolyl-NHC ligand, and the sixth position by a closely linear vinylidene chain Ru(1)-C(20)-C(21) , $174.9(2)^\circ$. This ligand exhibits a short Ru(1)-C(20) distance of $1.805(2)$ Å, which reflects the strong back-bonding from the metal characteristic of the vinylidene ligands. These data are comparable to those found for the closely related vinylidene complex $[\text{TpRu}\{\text{=C=C(OMe)Ph}\}(\kappa^2\text{-P,N-P}^i\text{Pr}_2\text{SPy})][\text{BAR}^{\text{F}}_4]^{16\text{a}}$. Examination of the bond distances in the coordination sphere of ruthenium reveals that the strongest trans influences are carried out by the C atoms of the vinylidene and NHC ligands.

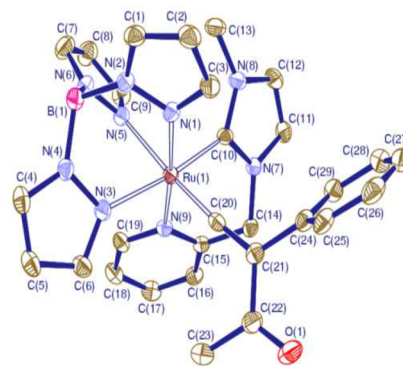


Figure 3. ORTEP view of the cation of $[\text{TpRu}\{\text{=C=C(OMe)Ph}\}(\kappa^2\text{-C,N-picolyl-MeI})][\text{BAR}^{\text{F}}_4]$ (**6a**). Selected bond lengths (Å) and angles (degrees): Ru(1)-N(1) 2.082(2), Ru(1)-N(3) 2.141(2), Ru(1)-N(5) 2.183(2), Ru(1)-N(9) 2.113(2), Ru(1)-C(10) 2.034(3), Ru(1)-C(20) 1.818(3), C(20)-C(21) 1.335(4), O(1)-C(22) 1.219(4); N(1)-Ru(1)-N(9) $174.01(8)^\circ$, N(3)-Ru(1)-C(10) $171.33(9)^\circ$, N(5)-Ru(1)-C(20) $175.61(10)^\circ$, Ru(1)-C(20)-C(21) $174.9(2)^\circ$, O(1)-C(22)-C(23) $121.4(3)^\circ$.

According to several reported theoretical studies,^{16,18,19,22} it is reasonable to assume that a π -alkyne intermediate is required in order to complete the isomerization process. The reaction mechanism must proceed via a direct 1,2-acyl shift from a nondetected π -alkyne complex.

The reaction of **1** with other disubstituted alkynes $\text{RC}\equiv\text{CR}'$ ($\text{R}, \text{R}' = \text{Ph}, \text{Ph}, \text{Me}, \text{CO}_2\text{Et}, \text{CO}_2\text{Et}$) did not lead to isolation of clean products. Several reaction conditions (i.e., temperature, time, and solvents) were attempted, but in all cases an uncharacterizable mixture of products was obtained.

It is interesting to note the differences in reactivity observed whether methyl 3-arylpropiolates or alkynones are used as substrates. One plausible explanation might be found in the stability of the reaction intermediates. In our previous work, while studying the activation of internal alkynes with $[\text{TpRu}(\kappa^2\text{-P,N-PyCH}_2\text{P}^i\text{Pr}_2)\text{-Cl}]$ it was evident that the presence of a ketone group in the alkyne increased the secondary vinylidene formation rate ($-\text{COMe} \gg -\text{COOMe}$).^{16a} Thus, formation of the disubstituted vinylidene might be less favored when methyl 3-arylpropiolates are used as substrates. Furthermore, given the experimental findings, it is plausible to assume that when $[\text{TpRu}(\kappa^2\text{-C,N-picolyl-MeI})\text{-Cl}]$ **1** and **2** are used as starting complexes the energy difference between the reaction intermediates that generate the secondary vinylidenes increases, leading to a new reaction pathway for activation of methyl 3-arylpropiolates. Also, intermediate **B** proposed in the reaction mechanism (Scheme 2) and its subsequent rearrangement is favored by the presence of the more electron donating $-\text{COOMe}$ group instead of the $-\text{COMe}$ group. Also, it is important to consider that the electronic effects might not be the only ones ruling this unusual transformation. Therefore, it is possible that the intermediate from reaction with methyl 3-arylpropiolates adopts a conformation where the NHC carbon orbitals are angled toward the alkyne orbitals, which will lead to an effective overlap and following nucleophilic attack.

CONCLUSIONS

The increasing importance of the field of internal alkynes activation and its application in several catalytic transformations has attracted our attention^{16–18} and led us to study the activation of these substrates with mononuclear ruthenium–

NHC complexes. In this work, we analyzed how different modifications affect this transformation, namely, (a) the picolyl-NHC ligand instead of the widely used phosphines and (b) the alkyne substituents with and without ketone groups.

Here, we reported an unprecedented C–N bond activation of a chelating NHC and migratory insertion of an NHC into a ruthenium–carbon bond. Our experimental findings revealed that under mild conditions a rare process of Ru–C_{NHC} bond cleavage and further attack into a feasible π -alkyne intermediate takes place, leading to C–N activation and tautomerization of a chelating NHC upon rearrangement of the reaction intermediate. The process is particularly interesting given the nature of the picolyl-NHC ligand, because the other tautomerization processes documented have been observed with monodentate NHCs.^{5,9,10} This is another example of the noninnocent behavior of NHC ligands.

It is particularly, interesting that this unusual reaction takes place with methyl 3-arylpropiolates, possibly because the intermediates needed for generation of the disubstituted vinylidenes are less favored and a new reaction pathway is preferred that enables nucleophilic attack of the NHC on the Ru–C bond. However, we cannot exclude the involvement of conformational factors in this transformation.

Furthermore, we reported that keto alkynes undergo an activation process to generate the corresponding secondary vinylidenes when the TpRu picolyl-NHC complexes are involved.

In summary, study of the activation of internal alkynes by picolyl-NHC ruthenium complexes revealed that significant differences are observed in comparison with the phosphine analogues.¹⁶ Particularly, use of methyl 3-arylpropiolates as substrates led to an unprecedented reaction that gives more insights into the nonspectator behavior of NHCs. A better overall understanding of the decomposition pathways of NHCs and the factors controlling the internal alkyne activation process should improve the design of metal complexes for catalytic transformations of these substrates.

EXPERIMENTAL SECTION

Unless otherwise stated, all manipulations were carried out under dry nitrogen or argon using conventional Schlenk techniques. Petroleum ether (boiling point range 40–60 °C) and diethyl ether were obtained oxygen and water free from an Innovative Technology Inc. solvent purification apparatus. Fluorobenzene was of anhydrous quality and used as received. All solvents were degassed immediately prior to use. $\text{TpRu}(\kappa^2\text{-C,N-3-(methyl)-1-(2-picolyl)imidazol-2-ylidene})\text{Cl}$ (**1**), $\text{TpRu}(\kappa^2\text{-C,N-3-(methyl)-1-(2-picolyl)benzoimidazol-2-ylidene})\text{Cl}$ (**2**), and $[\{\text{TpRu}(\kappa^2\text{-C,N-3-(methyl)-1-(2-picolyl)imidazol-2-ylidene})\}_2(\mu\text{-N}_2)][\text{BAR}^{\text{F}}_4]_2$ (**5**) were prepared according to previously published methods.⁷ $\text{NaBAR}^{\text{F}}_4$ ²³ and methyl 3-(4-trifluorophenyl)propiolate²⁴ were prepared using slightly modified versions of the published procedures. All other reagents were purchased from commercial sources and used without further purification.

NMR spectra were recorded using a Varian INOVA 400 MHz, Agilent 400 MHz, or Varian Inova 600 MHz spectrometer. Chemical shifts are reported relative to tetramethylsilane, $\text{Si}(\text{CH}_3)_4$, for ^1H and $^{13}\text{C}\{^1\text{H}\}$ and CFCl_3 for ^{19}F . Assignments of ^1H and $^{13}\text{C}\{^1\text{H}\}$ NMR spectra were made on the basis of 2D NMR experiments. Microanalyses were performed with a LECO CHNS-932 elemental analyzer by Servicios Centrales de Ciencia y Tecnología, Universidad de Cádiz.

$[\text{TpRu}(\kappa^3\text{-C,N,N'-1-phenyl-2-(1-methyl-1H-imidazol-2-yl)-3-pyridyl-prop-1-ylidene-2-carboxylic Acid Methyl Ester})]\text{BAR}^{\text{F}}_4$ (**3a**). $[\text{TpRu}(\text{picolyl-Me}^{\text{BI}})\text{Cl}]$ (130.6 mg, 0.25 mmol), methyl 3-phenylpropiolate (39 μL , 0.26 mmol), and $\text{NaBAR}^{\text{F}}_4$ (221.5 mg, 0.25

mmol) were suspended in 10 mL of fluorobenzene. An immediate color change to from red to green was observed. The solution was stirred at room temperature for 3 h, and the resulting green suspension was filtered through a pad of Celite to remove NaCl. Solvent was removed under vacuum; the residue was washed with petroleum ether (2 \times 10 mL) and dried to yield a green solid. Solid was recrystallized by layering from CH_2Cl_2 /pentane. Yield: 305.7 mg, 81%. ^1H NMR (CD_2Cl_2 , 600 MHz): δ 8.21 (d, $^3J_{\text{HH}} = 2.09$ Hz, 1H, H_{Tp}), 8.02 (d, $^3J_{\text{HH}} = 2.26$ Hz, 1H, H_{Tp}), 7.90 (d, $^3J_{\text{HH}} = 2.26$ Hz, 1H, H_{Tp}), 7.81 (br s, 8H, BAR^{F}_4), 7.77 (d, $^3J_{\text{HH}} = 1.75$ Hz, 1H, H_{Tp}), 7.62 (br s, 4H, BAR^{F}_4), 7.52 (m, 3H, $\text{H}_{\text{Ph}} + 2\text{H}_{\text{pyridine}}$), 7.21 (d, $^3J_{\text{HH}} = 5.93$ Hz, 1H, $\text{H}_{\text{pyridine}}$), 7.05 (t, $^3J_{\text{HH}} = 7.76$ Hz, 2H, H_{Ph}), 6.93 (d, $^3J_{\text{HH}} = 8.02$ Hz, 2H, H_{Ph}), 6.87 (s, 1H, H_{imid}), 6.81 (m, 1H, $\text{H}_{\text{pyridine}}$), 6.62 (vt, $^3J_{\text{HH}} = 1.83$ Hz, 1H, H_{Tp}), 6.51 (d, $^3J_{\text{HH}} = 0.70$ Hz, 1H, H_{imid}), 6.13 (vt, $^3J_{\text{HH}} = 2.09$ Hz, 1H, H_{Tp}), 6.08 (d, $^3J_{\text{HH}} = 1.74$ Hz, 1H, H_{Tp}), 5.83 (vt, $^3J_{\text{HH}} = 2.18$ Hz, 1H, H_{Tp}), 5.48 (d, $^3J_{\text{HH}} = 1.74$ Hz, 1H, H_{Tp}), 4.86 (d, $^2J_{\text{HH}} = 18.82$ Hz, 1H, H_{bridge}), 4.31 (d, $^2J_{\text{HH}} = 19.00$ Hz, 1H, H_{bridge}), 3.86 (s, 3H, NCH_3), 3.72 (s, 3H, OCH_3). $^{13}\text{C}\{^1\text{H}\}$ NMR (CD_2Cl_2 , 150 MHz): δ 329.3 (Ru=C), 171.4 (C=O), 162.3 (q, $^1J_{\text{B-C}} = 49.76$ Hz, BAR^{F}_4), 158.1 (C_{py}), 154.0 (Ph), 153.8 (C_{py}), 147.7 (C_{imid}), 143.7 (Tp), 143.8 (Tp), 143.0 (Tp), 137.6 (Tp), 137.5 (C_{py}), 137.5 (Tp), 136.8 (Tp), 135.3 (BAR^{F}_4), 131.5 (Ph), 129.4 (q, $^2J_{\text{C-F}} = 31.47$ Hz, BAR^{F}_4), 128.9 (Ph), 127.3 (C_{imid}), 127.1 (C_{py}), 125.2 (C_{imid}), 125.1 (q, $^1J_{\text{C-F}} = 272.21$ Hz, BAR^{F}_4), 123.6 (Ph), 123.4 (C_{py}), 118.0 (BAR^{F}_4), 108.0 (Tp), 107.2 (Tp), 106.7 (Tp), 75.7 (C_q), 54.0 (OCH_3), 41.4 (CH_2), 34.8 (NCH_3). Anal. Calcd for $\text{C}_{61}\text{H}_{41}\text{B}_2\text{F}_{24}\text{N}_9\text{O}_2\text{Ru}$: C, 48.50; H, 2.74; N, 8.34. Found: C, 48.46; H, 2.80; N, 8.32.

$[\text{TpRu}(\kappa^3\text{-C,N,N'-1-(4-trifluoromethylphenyl)-2-(1-methyl-1H-imidazol-2-yl)-3-pyridyl-prop-1-ylidene-2-carboxylic Acid Methyl Ester})]\text{BAR}^{\text{F}}_4$ (**3b**). $[\text{TpRu}(\text{picolyl-Me}^{\text{BI}})\text{Cl}]$ (130.6 mg, 0.25 mmol), methyl 3-(4-trifluoromethylphenyl)propiolate (59.3 mg, 0.26 mmol), and $\text{NaBAR}^{\text{F}}_4$ (221.5 mg, 0.25 mmol) were suspended in 10 mL of fluorobenzene. An immediate color change to from red to green was observed. The solution was stirred at room temperature for 3 h, and the resulting green suspension was filtered through a pad of Celite to remove NaCl. Solvent was removed under vacuum; the residue was washed with petroleum ether (2 \times 10 mL) and dried to yield a green solid. The solid was recrystallized by layering from CH_2Cl_2 /pentane. Yield: 347.5 mg, 88%. ^1H NMR (CD_2Cl_2 , 400 MHz): δ 8.18 (d, $^3J_{\text{HH}} = 1.96$ Hz, 1H, H_{Tp}), 7.99 (d, $^3J_{\text{HH}} = 2.44$ Hz, 1H, H_{Tp}), 7.87 (d, $^3J_{\text{HH}} = 2.45$ Hz, 1H, H_{Tp}), 7.72 (br s, 9H, $\text{BAR}^{\text{F}}_4 + \text{H}_{\text{Tp}}$), 7.56 (br s, 4H, BAR^{F}_4), 7.54 (d, $^3J_{\text{HH}} = 7.11$ Hz, 1H, $\text{H}_{\text{pyridine}}$), 7.51 (t, $^3J_{\text{HH}} = 8.00$ Hz, 1H, $\text{H}_{\text{pyridine}}$), 7.26 (d, $^3J_{\text{HH}} = 8.32$ Hz, 2H, H_{Ph}), 7.01 (d, $^3J_{\text{HH}} = 5.92$ Hz, 1H, $\text{H}_{\text{pyridine}}$), 6.97 (d, $^3J_{\text{HH}} = 8.31$ Hz, 2H, H_{Ph}), 6.87 (d, $^3J_{\text{HH}} = 1.46$ Hz, 1H, H_{imid}), 6.81 (t, $^3J_{\text{HH}} = 6.60$ Hz, 1H, $\text{H}_{\text{pyridine}}$), 6.60 (vt, $^3J_{\text{HH}} = 1.96$ Hz, 1H, H_{Tp}), 6.43 (d, $^3J_{\text{HH}} = 1.96$ Hz, 1H, H_{imid}), 6.11 (vt, $^3J_{\text{HH}} = 1.96$ Hz, 1H, H_{Tp}), 5.98 (d, $^3J_{\text{HH}} = 1.95$ Hz, 1H, H_{Tp}), 5.80 (vt, $^3J_{\text{HH}} = 2.45$ Hz, 1H, H_{Tp}), 5.36 (d, $^3J_{\text{HH}} = 1.47$ Hz, 1H, H_{Tp}), 4.80 (d, $^2J_{\text{HH}} = 19.07$ Hz, 1H, H_{bridge}), 4.24 (d, $^2J_{\text{HH}} = 18.58$ Hz, 1H, H_{bridge}), 3.83 (s, 3H, NCH_3), 3.67 (s, 3H, OCH_3). $^{13}\text{C}\{^1\text{H}\}$ NMR (CD_2Cl_2 , 100 MHz): δ 326.9 (Ru=C), 170.7 (C=O), 162.1 (q, $^1J_{\text{B-C}} = 49.59$ Hz, BAR^{F}_4), 157.7 (C_{py}), 155.7 (Ph), 153.7 (C_{py}), 147.1 (C_{imid}), 143.6 (Tp), 143.4 (Tp), 142.7 (Tp), 137.8 (Tp), 137.8 (C_{py}), 137.6 (Tp), 137.1 (Tp), 135.2 (BAR^{F}_4), 133.5 (q, $^2J_{\text{C-F}} = 33.10$ Hz, Ph), 129.2 (q, $^2J_{\text{C-F}} = 31.19$ Hz, BAR^{F}_4), 127.2 (C_{py}), 127.1 (C_{imid}), 125.9 (Ph), 125.8 (C_{imid}), 124.9 (q, $^1J_{\text{C-F}} = 272.75$ Hz, BAR^{F}_4), 123.6 (C_{py}), 123.0 (Ph), 117.8 (BAR^{F}_4), 108.2 (Tp), 107.3 (Tp), 106.9 (Tp), 76.3 (C_q), 54.3 (OCH_3), 41.0 (CH_2), 34.9 (NCH_3). ^{19}F NMR (CD_2Cl_2 , 376 MHz, CFCl_3): δ -62.87 (BAR^{F}_4), -63.97 (PhCF_3). Anal. Calcd for $\text{C}_{62}\text{H}_{40}\text{B}_2\text{F}_{27}\text{N}_9\text{O}_2\text{Ru}$: C, 47.17; H, 2.55; N, 7.99. Found: C, 47.20; H, 2.59; N, 7.96.

$[\text{TpRu}(\kappa^3\text{-C,N,N'-1-phenyl-2-(1-methyl-1H-benzoimidazol-2-yl)-3-pyridyl-prop-1-ylidene-2-carboxylic Acid Methyl Ester})]\text{BAR}^{\text{F}}_4$ (**4a**). $[\text{TpRu}(\text{picolyl-Me}^{\text{BI}})\text{Cl}]$ (143.2 mg, 0.25 mmol), methyl 3-phenylpropiolate (39 μL , 0.26 mmol), and $\text{NaBAR}^{\text{F}}_4$ (221.5 mg, 0.25 mmol) were suspended in 10 mL of fluorobenzene. An immediate color change from red to brown was observed. The solution was stirred overnight at 40 °C, and the resulting brown suspension was filtered through a pad of Celite to remove NaCl. Solvent was removed under vacuum; the residue was washed with petroleum ether (2 \times 10

mL) and dried to yield a brown solid. Solid was recrystallized by layering from CH_2Cl_2 /pentane. Yield: 308.2 mg, 79%. ^1H NMR (CD_3NO_2 , 400 MHz): δ 8.34 (d, $^3J_{\text{HH}} = 1.95$ Hz, 1H, H_{TP}), 8.13 (d, $^3J_{\text{HH}} = 1.47$ Hz, 1H, H_{TP}), 7.95 (d, $^3J_{\text{HH}} = 1.96$ Hz, 1H, H_{TP}), 7.93 (d, $^3J_{\text{HH}} = 1.47$ Hz, 1H, H_{TP}), 7.87 (br s, 8H, BAR^{F}_4), 7.67 (br s, 5H, $\text{BAR}^{\text{F}}_4 + \text{H}_{\text{pyridine}}$), 7.62 (m, 2H, $\text{H}_{\text{pyridine}} + \text{H}_{\text{benzoimid}}$), 7.50 (t, $^3J_{\text{HH}} = 7.09$ Hz, 1H, H_{Ph}), 7.32 (m, 1H, $\text{H}_{\text{benzoimid}}$), 7.26 (d, $^3J_{\text{HH}} = 5.37$ Hz, 1H, $\text{H}_{\text{pyridine}}$), 7.03 (m, 5H, $\text{H}_{\text{Ph}} + \text{H}_{\text{benzoimid}}$), 6.86 (t, $^3J_{\text{HH}} = 6.48$ Hz, 1H, $\text{H}_{\text{pyridine}}$), 6.66 (d, $^3J_{\text{HH}} = 2.07$ Hz, 1H, H_{TP}), 6.64 (d, $^3J_{\text{HH}} = 8.05$ Hz, 1H, $\text{C}_{\text{benzoimid}}$), 6.10 (m, 2H, H_{TP}), 5.82 (vt, $^3J_{\text{HH}} = 1.96$ Hz, 1H, H_{TP}), 5.66 (d, $^3J_{\text{HH}} = 1.46$ Hz, 1H, H_{TP}), 5.14 (d, $^2J_{\text{HH}} = 19.08$ Hz, 1H, H_{bridge}), 4.69 (d, $^2J_{\text{HH}} = 19.08$ Hz, 1H, H_{bridge}), 4.15 (s, 3H, NCH_3), 3.72 (s, 3H, OCH_3). $^{13}\text{C}\{^1\text{H}\}$ NMR (CD_3NO_2 , 100 MHz): δ 331.1 (Ru=C), 172.1 (C=O), 163.1 (q, $^1J_{\text{B-C}} = 49.85$ Hz, BAR^{F}_4), 159.7 (C_{py}), 155.7 ($\text{C}_{\text{benzoimid}}$), 154.8 (C_{py}), 154.5 (Ph), 146.8 (Tp), 144.8 (Tp), 144.0 (Tp), 140.6 ($\text{C}_{\text{benzoimid}}$), 138.7 (Tp), 138.5 (C_{py}), 138.4 (Tp), 137.8 ($\text{C}_{\text{benzoimid}}$), 137.6 (Tp), 136.2 (BAR^{F}_4), 131.9 (Ph), 130.3 (q, $^2J_{\text{C-F}} = 31.15$ Hz, BAR^{F}_4), 129.5 (Ph), 128.1 (C_{py}), 126.0 (q, $^1J_{\text{C-F}} = 271.51$ Hz, BAR^{F}_4), 125.6 ($\text{C}_{\text{benzoimid}}$), 124.7 (C_{py}), 124.2 (Ph), 118.9 (BAR^{F}_4), 117.9 ($\text{C}_{\text{benzoimid}}$), 112.8 ($\text{C}_{\text{benzoimid}}$), 108.2 (Tp), 108.0 (Tp), 107.4 (Tp), 78.0 (C_q), 54.6 (OCH_3), 41.7 (CH_2), 32.2 (NCH_3). Anal. Calcd for $\text{C}_{65}\text{H}_{43}\text{B}_2\text{F}_{24}\text{N}_9\text{O}_2\text{Ru}$: C, 50.27; H, 3.00; N, 7.99. Found: C, 50.19; H, 3.05; N, 8.07.

[TpRu(κ^2 -C,N,N'-1-(4-trifluoromethylphenyl)-2-(1-methyl-1H-benzimidazol-2-yl)-3-pyridyl-prop-1-ylidene-2-carboxylic Acid Methyl Ester)]BAR $^{\text{F}}_4$ (4b). [TpRu(picolyl- $^{\text{Me}}\text{BI}$)Cl] (143.2 mg, 0.25 mmol), methyl 3-(4-trifluoromethylphenyl)propionate (59.3 mg, 0.26 mmol), and NaBAR $^{\text{F}}_4$ (221.5 mg, 0.25 mmol) were suspended in 10 mL of fluorobenzene. An immediate color change to from red to brown was observed. The solution was stirred overnight at 40 °C, and the resulting green-brown suspension was filtered through a pad of Celite to remove NaCl. Solvent was removed under vacuum; the residue was washed with petroleum ether (2 \times 10 mL) and dried to yield a brown solid. Solid was recrystallized by layering from CH_2Cl_2 /pentane. Yield: 346.1 mg, 85%. ^1H NMR (CD_3NO_2 , 400 MHz): δ 8.37 (d, $^3J_{\text{HH}} = 2.11$ Hz, 1H, H_{TP}), 8.17 (d, $^3J_{\text{HH}} = 2.03$ Hz, 1H, H_{TP}), 7.96 (d, $^3J_{\text{HH}} = 2.62$ Hz, 1H, H_{TP}), 7.94 (d, $^3J_{\text{HH}} = 2.73$ Hz, 1H, H_{TP}), 7.85 (br s, 8H, BAR^{F}_4), 7.67 (br s, 4H, BAR^{F}_4), 7.64 (m, 2H, $\text{H}_{\text{pyridine}} + \text{H}_{\text{benzoimid}}$), 7.36 (m, 4H, $\text{H}_{\text{pyridine}} + \text{H}_{\text{benzoimid}} + \text{H}_{\text{Ph}}$), 7.22 (d, $^3J_{\text{HH}} = 5.74$ Hz, 1H, $\text{H}_{\text{pyridine}}$), 7.15 (d, $^3J_{\text{HH}} = 8.14$ Hz, 2H, H_{Ph}), 7.07 (t, $^3J_{\text{HH}} = 7.50$ Hz, 1H, $\text{H}_{\text{benzoimid}}$), 6.92 (t, $^3J_{\text{HH}} = 6.47$ Hz, 1H, $\text{H}_{\text{pyridine}}$), 6.69 (vt, $^3J_{\text{HH}} = 2.11$ Hz, 1H, Tp), 6.63 (d, $^3J_{\text{HH}} = 8.29$ Hz, 1H, $\text{H}_{\text{benzoimid}}$), 6.13 (vt, $^3J_{\text{HH}} = 2.22$ Hz, 1H, H_{TP}), 6.09 (d, $^3J_{\text{HH}} = 1.50$ Hz, 1H, H_{TP}), 5.83 (vt, $^3J_{\text{HH}} = 2.24$ Hz, 1H, H_{TP}), 5.66 (d, $^3J_{\text{HH}} = 2.00$ Hz, 1H, H_{TP}), 5.17 (d, $^2J_{\text{HH}} = 19.11$ Hz, 1H, H_{bridge}), 4.68 (d, $^2J_{\text{HH}} = 19.14$ Hz, 1H, H_{bridge}), 4.16 (s, 3H, NCH_3), 3.71 (s, 3H, OCH_3). $^{13}\text{C}\{^1\text{H}\}$ NMR (CD_3NO_2 , 100 MHz): δ 329.2 (Ru=C), 171.5 (C=O), 163.2 (q, $^1J_{\text{B-C}} = 50.23$ Hz, BAR^{F}_4), 159.6 (C_{py}), 158.4 (Ph), 154.7 (C_{py}), 154.1 ($\text{C}_{\text{benzoimid}}$), 146.9 (Tp), 144.7 (Tp), 143.9 (Tp), 140.5 ($\text{C}_{\text{benzoimid}}$), 138.9 (Tp), 138.8 (C_{py}), 138.5 (Tp), 137.8 (Tp), 137.8 ($\text{C}_{\text{benzoimid}}$), 136.2 (BAR^{F}_4), 131.6 (q, $^2J_{\text{C-F}} = 32.93$ Hz, Ph), 130.2 (q, $^2J_{\text{C-F}} = 31.57$ Hz, BAR^{F}_4), 128.2 (C_{py}), 127.0 (Ph), 126.5 ($\text{C}_{\text{benzoimid}}$), 126.4 (Ph), 126.0 (q, $^1J_{\text{C-F}} = 271.89$ Hz, BAR^{F}_4), 125.7 (Ph), 124.8 ($\text{C}_{\text{benzoimid}}$), 124.4 (C_{py}), 123.6 (Ph), 119.0 (BAR^{F}_4), 117.8 ($\text{C}_{\text{benzoimid}}$), 112.9 ($\text{C}_{\text{benzoimid}}$), 108.3 (Tp), 108.1 (Tp), 107.5 (Tp), 78.7 (C_q), 54.8 (OCH_3), 41.6 (CH_2), 32.3 (NCH_3). ^{19}F NMR (CD_3NO_2 , 376 MHz, CFCl_3): δ -63.52 (BAR^{F}_4), -64.38 (PhCF $_3$). Anal. Calcd for $\text{C}_{66}\text{H}_{42}\text{B}_2\text{F}_{27}\text{N}_9\text{O}_2\text{Ru}$: C, 48.67; H, 2.60; N, 7.74. Found: C, 47.20; H, 2.59; N, 7.96.

[TpRu(κ^2 -C,N-3-(methyl)-1-(2-picolyl)imidazol-2-ylidene)](C=C(COMe)Ph)]BAR $^{\text{F}}_4$ (6a). [TpRu(picolyl- $^{\text{Me}}\text{I}$)Cl] (105.5 mg, 0.2 mmol) and NaBAR $^{\text{F}}_4$ (177.2 mg, 0.2 mmol) were suspended in 6 mL of fluorobenzene. After these reagents were completely dissolved (~1–2 min), 4-phenyl-3-butanone (34 μL , 0.26 mmol) was added, causing an immediate color change from red to brown. The solution was stirred overnight at room temperature. The resulting solution was filtered through a pad of Celite to remove NaCl. Solvent was removed under vacuum; the residue was washed with petroleum ether (2 \times 10 mL) and dried to yield a red-brown solid. Solid was recrystallized by layering from CH_2Cl_2 /pentane. Yield: 251.2 mg, 84%. ^1H NMR

(CD_2Cl_2 , 400 MHz): δ 7.95 (d, $^3J_{\text{HH}} = 2.31$ Hz, 1H, H_{TP}), 7.90 (t, $^3J_{\text{HH}} = 7.39$ Hz, 1H, $\text{H}_{\text{pyridine}}$), 7.88 (d, $^3J_{\text{HH}} = 2.44$ Hz, 1H, H_{TP}), 7.85 (d, $^3J_{\text{HH}} = 2.43$ Hz, 1H, H_{TP}), 7.72 (br s, 8H, BAR^{F}_4), 7.63 (d, $^3J_{\text{HH}} = 7.95$ Hz, 1H, $\text{H}_{\text{pyridine}}$), 7.55 (br s, 5H, $\text{BAR}^{\text{F}}_4 + \text{H}_{\text{pyridine}}$), 7.32 (d, $^3J_{\text{HH}} = 2.05$ Hz, 1H, H_{TP}), 7.31 (d, $^3J_{\text{HH}} = 2.05$ Hz, 1H, H_{imid}), 7.26 (m, 1H, H_{Ph}), 7.22 (m, 2H, H_{Ph}), 7.14 (t, $^3J_{\text{HH}} = 6.54$ Hz, 1H, $\text{H}_{\text{pyridine}}$), 6.96 (d, $^3J_{\text{HH}} = 2.05$ Hz, 1H, H_{imid}), 6.93 (d, $^3J_{\text{HH}} = 2.05$ Hz, 1H, H_{TP}), 6.71 (m, 2H, H_{Ph}), 6.41 (d, $^3J_{\text{HH}} = 1.79$ Hz, 1H, H_{TP}), 6.26 (vt, $^3J_{\text{HH}} = 2.30$ Hz, 1H, H_{TP}), 6.22 (vt, $^3J_{\text{HH}} = 2.31$ Hz, 1H, H_{TP}), 6.20 (vt, $^3J_{\text{HH}} = 2.18$ Hz, 1H, H_{TP}), 6.15 (d, $^2J_{\text{HH}} = 15.64$ Hz, 1H, H_{bridge}), 5.19 (d, $^2J_{\text{HH}} = 15.64$ Hz, 1H, H_{bridge}), 2.38 (s, 3H, NCH_3), 1.95 (s, 3H, CH_3). $^{13}\text{C}\{^1\text{H}\}$ NMR (CD_2Cl_2 , 100 MHz): δ 354.7 (Ru=C), 194.6 (C=O), 172.3 ($\text{C}_{\text{imid}}\text{Ru}$), 161.1 (q, $^1J_{\text{B-C}} = 49.72$ Hz, BAR^{F}_4), 156.2 (C_{py}), 155.6 (C_{py}), 146.4 (Tp), 144.2 (Tp), 142.0 (Tp), 140.2 (C_{py}), 137.8 (Tp), 137.2 (Tp), 137.0 (Tp), 135.4 (Ph), 135.2 (BAR^{F}_4), 130.8 (Ph), 129.4 (Ph), 129.2 (q, $^2J_{\text{C-F}} = 31.60$ Hz, BAR^{F}_4), 128.6 (Ph), 125.7 (C_{py}), 125.6 (C_{py}), 124.7 (q, $^1J_{\text{C-F}} = 272.24$ Hz, BAR^{F}_4), 124.7 (Ru=C), 122.7 (C_{imid}), 117.9 (BAR^{F}_4), 107.8 (Tp), 107.6 (Tp), 107.5 (Tp), 56.5 (CH_2), 36.1 (NCH_3), 30.4 (CH_3). Anal. Calcd for $\text{C}_{61}\text{H}_{41}\text{B}_2\text{F}_{24}\text{N}_9\text{ORu}$: C, 49.02; H, 2.76; N, 8.43. Found: C, 49.05; H, 2.81; N, 8.38.

[TpRu(κ^2 -C,N-3-(methyl)-1-(2-picolyl)imidazol-2-ylidene)](C=C(COPh)Ph)]BAR $^{\text{F}}_4$ (6b). [TpRu(picolyl- $^{\text{Me}}\text{I}$)Cl] (130.6 mg, 0.25 mmol), 1,3-diphenylprop-2-yn-1-one (67.1 mg, 0.32 mmol), and NaBAR $^{\text{F}}_4$ (221.5 mg, 0.25 mmol) were suspended in 10 mL of fluorobenzene. An immediate color change from red to brown was observed. The solution was stirred overnight at room temperature, and the resulting brown suspension was filtered through a pad of Celite to remove NaCl. Solvent was removed under vacuum; the residue was washed with petroleum ether (2 \times 10 mL) and dried to yield a brown solid. Solid was recrystallized by layering from CH_2Cl_2 /pentane. Yield: 299.8 mg, 77%. ^1H NMR (CD_2Cl_2 , 600 MHz): δ 7.94 (t, $^3J_{\text{HH}} = 7.67$ Hz, 1H, $\text{H}_{\text{pyridine}}$), 7.89 (d, $^3J_{\text{HH}} = 2.30$ Hz, 1H, H_{TP}), 7.84 (d, $^3J_{\text{HH}} = 2.49$ Hz, 1H, H_{TP}), 7.76 (d, $^3J_{\text{HH}} = 2.49$ Hz, 1H, H_{TP}), 7.73 (br s, 9H, $\text{BAR}^{\text{F}}_4 + \text{H}_{\text{pyridine}}$), 7.56 (br s, 4H, BAR^{F}_4), 7.47 (d, $^3J_{\text{HH}} = 7.48$ Hz, 2H, H_{Ph}), 7.41 (d, $^3J_{\text{HH}} = 1.92$ Hz, 1H, H_{imid}), 7.37 (m, 2H, $\text{H}_{\text{Ph}} + \text{H}_{\text{pyridine}}$), 7.22 (m, 3H, H_{Ph}), 7.12 (t, $^3J_{\text{HH}} = 7.10$ Hz, 1H, $\text{H}_{\text{pyridine}}$), 7.00 (m, 5H, $\text{H}_{\text{Ph}} + \text{H}_{\text{imid}}$), 6.70 (vt, $^3J_{\text{HH}} = 2.59$ Hz, 1H, H_{TP}), 6.42 (d, $^2J_{\text{HH}} = 15.73$ Hz, 1H, H_{bridge}), 6.35 (d, $^3J_{\text{HH}} = 2.11$ Hz, 1H, H_{TP}), 6.19 (vt, $^3J_{\text{HH}} = 2.21$ Hz, 1H, H_{TP}), 6.15 (vt, $^3J_{\text{HH}} = 2.48$ Hz, 1H, H_{TP}), 6.00 (vt, $^3J_{\text{HH}} = 2.21$ Hz, 1H, H_{TP}), 5.94 (vt, $^3J_{\text{HH}} = 2.31$ Hz, 1H, H_{TP}), 5.40 (d, $^2J_{\text{HH}} = 15.54$ Hz, 1H, H_{bridge}), 2.27 (s, 3H, NCH_3). $^{13}\text{C}\{^1\text{H}\}$ NMR (CD_2Cl_2 , 150 MHz): δ 353.1 (Ru=C), 189.2 (C=O), 172.6 ($\text{C}_{\text{imid}}\text{Ru}$), 162.2 (q, $^1J_{\text{B-C}} = 49.92$ Hz, BAR^{F}_4), 156.4 (C_{py}), 155.7 (C_{py}), 146.5 (Tp), 144.0 (Tp), 142.2 (Ph), 142.1 (Tp), 140.3 (C_{py}), 137.8 (Tp), 137.1 (Tp), 136.7 (Tp), 135.2 (BAR^{F}_4), 133.3 (Ph), 132.9 (Ph), 129.6 (Ph), 129.4 (Ph), 129.3 (q, $^2J_{\text{C-F}} = 31.97$ Hz, BAR^{F}_4), 128.5 (Ph), 128.4 (Ph), 128.3 (Ph), 126.4 (Ru=C), 126.0 (C_{py}), 125.7 (C_{py}), 125.4 (q, $^1J_{\text{C-F}} = 272.58$ Hz, BAR^{F}_4), 124.9 (C_{imid}), 123.0 (C_{imid}), 117.9 (BAR^{F}_4), 107.8 (Tp), 107.5 (Tp), 107.4 (Tp), 56.5 (CH_2), 36.0 (NCH_3). Anal. Calcd for $\text{C}_{66}\text{H}_{43}\text{B}_2\text{F}_{24}\text{N}_9\text{ORu}$: C, 50.92; H, 2.78; N, 8.10. Found: C, 50.97; H, 2.82; N, 8.07.

Crystal Structure Analysis. Crystals of **3a**, **3b**, **6a**, and **6b** suitable for X-ray structural determination were mounted on glass fibers and then transferred to the cold nitrogen gas stream of a Bruker Smart APEX CCD three-circle diffractometer ($T = 100$ K) with a sealed-tube source and graphite-monochromated Mo $K\alpha$ radiation ($\alpha = 0.710$ 73 Å) at the Servicio Central de Ciencia y Tecnología de la Universidad de Cádiz. Four sets of frames were recorded over a hemisphere of the reciprocal space by ω scans with $\delta(\omega) = 0.30$ and an exposure of 10 s per frame. No significant decay was observed over the course of data collection. Intensity data were corrected for Lorentz and polarization effects and absorption corrections applied using SADABS.²⁵ Structures were solved by direct methods and refined on F^2 by full-matrix least-squares (SHELX97) using all unique data.²⁶ All non-hydrogen atoms were refined anisotropically with hydrogen atoms included in calculated positions (riding model). Some disordered CF_3 groups in the (BAR^{F}_4) $^-$ anion for **3a**, **3b**, **6a**, and **6b**, the CH_2Cl_2 solvate for **6a** and NHC, and partly vinylidene ligands for **6b** were refined split in two complementary orientations using displacement parameter

restraints. The program ORTEP-3 was used for plotting.²⁷ In the Supporting Information, Table S1 summarizes the crystal data and data collection and refinement details for **3a**, **3b**, **6a**, and **6b**.

■ ASSOCIATED CONTENT

■ Supporting Information

Kinetic data (integral vs time plots), rate constants table, and CIF files giving crystallographic data for compounds **3a**, **3b**, **6a**, and **6b**. This material is available free of charge via the Internet at <http://pubs.acs.org>.

■ AUTHOR INFORMATION

Corresponding Author

*E-mail: pedro.valerga@uca.es (P.V.); carmen.puerta@uca.es (M.d.C.P.).

Notes

The authors declare no competing financial interest.

■ ACKNOWLEDGMENTS

We thank the Spanish MICINN (Project CTQ2010-15390) and “Junta de Andalucía” (PAI-FQM188 and Project of Excellence P08-FQM-03538) for financial support and Johnson Matthey plc for generous loans of ruthenium trichloride. F.E.F. acknowledges the Spanish MICINN for a FPI fellowship (BES-2008-006635).

■ REFERENCES

- (1) Crabtree, R. H. *J. Organomet. Chem.* **2005**, *690*, 5451–5457.
- (2) (a) Díez-González, S.; Marion, N.; Nolan, S. P. *Chem. Rev.* **2009**, *109*, 3612–3676. (b) Hahn, F. E.; Jahnke, M. C. *Angew. Chem., Int. Ed.* **2008**, *47*, 3122–3172. (c) Nolan, S. P.; Clavier, H. *Annu. Rep. Prog. Chem., Sect. B* **2007**, *103*, 193–222. (d) Nolan, S. P. *N-Heterocyclic Carbenes in Synthesis*; Wiley-VCH: Weinheim, Germany, 2006. (e) Herrmann, W. A. *Angew. Chem., Int. Ed.* **2002**, *41*, 1290–1309. (f) Bourissou, D.; Guerret, O.; Gabbai, F. P.; Bertrand, G. *Chem. Rev.* **2000**, *100*, 39–91.
- (3) (a) Graham, D. C.; Cavell, K. J.; Yates, B. F. *Dalton Trans.* **2006**, 1768–1775. (b) Caddick, S.; Cloke, F. G. N.; Hitchcock, P. B.; Leonard, J.; Lewis, A. K. de K.; McKerrecher, D.; Titcomb, L. R. *Organometallics* **2002**, *21*, 4318–4319. (c) McGuinness, D. S.; Mueller, W.; Wasserscheid, P.; Cavell, K. J.; Skelton, B. W.; White, A. H.; Englert, U. *Organometallics* **2002**, *21*, 175–181. (d) McGuinness, D. S.; Saending, N.; Yates, B. F.; Cavell, K. J. *J. Am. Chem. Soc.* **2001**, *123*, 4029–4040.
- (4) (a) Segarra, C.; Mas-Marzá, E.; Benítez, M.; Mata, J. A.; Peris, E. *Angew. Chem., Int. Ed.* **2012**, *51*, 10841–10845. (b) Corberán, R.; Sanaú, M.; Peris, E. *J. Am. Chem. Soc.* **2006**, *128*, 3974–3979. (c) Corberán, R.; Sanaú, M.; Peris, E. *Organometallics* **2006**, *25*, 4002–4008. (d) Hanasha, F.; Tanabe, Y.; Fujita, K.; Yamaguchi, R. *Organometallics* **2006**, *25*, 826–831. (e) Scott, N. M.; Dorta, R.; Stevens, E. D.; Correa, A.; Cavallo, L.; Nolan, S. P. *J. Am. Chem. Soc.* **2005**, *127*, 3516–3526. (f) Scott, N. M.; Pons, V.; Stevens, E. D.; Nolan, S. P. *J. Am. Chem. Soc.* **2004**, *126*, 5054–5055. (g) Crudden, C. M.; Allen, D. P. *Coord. Chem. Rev.* **2004**, *248*, 2247–2273. (h) Jazzar, R. F. R.; Macgregor, S. A.; Mahon, M. F.; Whittlesey, M. K. *J. Am. Chem. Soc.* **2002**, *124*, 4944–4945.
- (5) (a) Wang, X.; Chen, H.; Li, X. *Organometallics* **2007**, *26*, 4684–4687. (b) Caddick, S.; Cloke, F. G. N.; Hitchcock, P. B.; Lewis, A. K. de K. *Angew. Chem., Int. Ed.* **2004**, *43*, 5824–5827.
- (6) For a comprehensive review of functionalized NHCs, see: (a) Cabeza, J. A.; Damonte, M.; García-Álvarez, P.; Kennedy, A. R.; Pérez-Carreño, E. *Organometallics* **2011**, *30*, 826–833. (b) Cross, E. D.; Bierenstiel, M. *Coord. Chem. Rev.* **2011**, *255*, 574–590. (c) Takaki, D.; Okayama, T.; Shuto, H.; Matsumoto, S.; Yamaguchi, Y.; Matsumoto, S. *Dalton Trans.* **2011**, 1445–1447. (d) Warsink, S.; Chang, I.; Weigand, J. J.; Hauwert, P.; Chen, J.; Elsevier, C. J. *Organometallics* **2010**, *29*, 4555–4561. (e) Amar, H. B.; Hassine, B. B.; Fischmeister, C.; Dixneuf, P. H.; Bruneau, C. *Eur. J. Inorg. Chem.* **2010**, 4752–4756. (f) Pažiký, M.; Loos, A.; Ferreira, M. J.; Serra, D.; Vinokurov, N.; Rominger, F.; Jäkel, C.; Hashmi, A. S. K.; Limbach, M. *Organometallics* **2010**, *29*, 4448–4458. (g) Hahn, F. E.; Naziruddin, A. R.; Hepp, A.; Pape, T. *Organometallics* **2010**, *29*, 5283–5288. (h) Makino, T.; Yamasaki, R.; Azumaya, I.; Masu, H.; Saito, S. *Organometallics* **2010**, *29*, 6291–6297. (i) Gandolfi, C.; Heckenroth, M.; Neels, A.; Laurenczy, G.; Albrecht, M. *Organometallics* **2009**, *28*, 5112–5121. (j) Downing, S. P.; Pogorzelec, P. J.; Danopoulos, A. A.; Cole-Hamilton, D. J. *Eur. J. Inorg. Chem.* **2009**, 1816–1824. (k) Binobaid, A.; Iglesias, M.; Beetstra, D. J.; Kariuki, B.; Dervisi, A.; Fallis, I. A.; Cavell, K. J. *Dalton Trans.* **2009**, 7099–7112. (l) Gnanamgari, D.; Sauer, E. L. O.; Schley, N. D.; Butler, C.; Incarvito, C. D.; Crabtree, R. H. *Organometallics* **2009**, *28*, 321–325. (m) Song, G.; Li, X.; Song, Z.; Zhao, J.; Zhang, H. *Chem.—Eur. J.* **2009**, *15*, 5535–5544. (n) Normand, A. T.; Cavell, K. J. *Eur. J. Inorg. Chem.* **2008**, 2781–2800. (o) Lee, C.; Ke, W.; Chan, K.; Lai, C.; Hu, C.; Lee, H. *Chem.—Eur. J.* **2007**, *13*, 582–591. (p) Nielsen, D. J.; Cavell, K. J.; Skelton, B. W.; White, A. H. *Organometallics* **2006**, *25*, 4850–4856.
- (7) Fernández, F. E.; Puerta, M. C.; Valerga, P. *Inorg. Chem.* **2013**, *58*, 4396–4410.
- (8) Fernández, F. E.; Puerta, M. C.; Valerga, P. *Organometallics* **2011**, *30*, 5793–5802.
- (9) (a) Sini, G.; Eisenstein, O.; Crabtree, R. H. *Inorg. Chem.* **2002**, *41*, 602–604. (b) Chianese, A. R.; Crabtree, R. H. In *Activation and Functionalization of C-H Bonds*; Goldberg, K. I., Goldman, A. S., Eds.; ACS Symposium Series 885; American Chemical Society: Washington, DC, 2004; pp 169–184.
- (10) (a) Hüller, L. J. L.; Page, M. J.; Erhardt, S.; Macgregor, S. A.; Mahon, M. F.; Naser, M. A.; Vélez, A.; Whittlesey, M. K. *J. Am. Chem. Soc.* **2010**, *132*, 18408–18416. (b) Burling, S.; Mahon, M. F.; Powell, R. E.; Whittlesey, M. K.; Williams, J. M. J. *J. Am. Chem. Soc.* **2006**, *128*, 13702–13703.
- (11) For reviews, see: (a) Lyman, J. M. *Chem.—Eur. J.* **2010**, *16*, 8238–8247. (b) In *Metal Vinylidenes and Allenylidenes in Catalysis: From Reactivity to Applications in Synthesis*; Bruneau, C.; Dixneuf, P. H., Eds.; Wiley-VCH: Weinheim, Germany, 2008. (c) Antonova, A. B. *Coord. Chem. Rev.* **2007**, *251*, 1521–1560. (d) Cadierno, V.; Gamasa, M. P.; Gimeno, J. *Coord. Chem. Rev.* **2004**, *248*, 1627–1657. (e) Wakatsuki, Y. *J. Organomet. Chem.* **2004**, *689*, 4092–4109. (f) Valerga, P.; Puerta, M. C. *Coord. Chem. Rev.* **1999**, *193*–195, 977–1025.
- (12) (a) Lass, R. W.; Werner, H. *Inorg. Chim. Acta* **2011**, *369*, 288–291. (b) Ilg, K.; Paneque, M.; Poveda, M. L.; Rendón, N.; Santos, L. L.; Carmona, E.; Mereiter, K. *Organometallics* **2006**, *25*, 2230–2236. (c) Konkol, M.; Steinborn, D. J. *Organomet. Chem.* **2006**, *691*, 2839–2845. (d) Jiménez, M. V.; Sola, E.; Lahoz, F. J.; Oro, L. A. *Organometallics* **2005**, *24*, 2722–2729. (e) Miura, T.; Murata, H.; Kiyota, K.; Kusama, H.; Iwasawa, N. *J. Mol. Catal. A: Chem.* **2004**, *213*, 59–71. (f) Murakami, M.; Hori, S. *J. Am. Chem. Soc.* **2003**, *125*, 4720–4721. (g) Huang, D.; Streib, W. E.; Eisenstein, O.; Caulton, K. G. *Organometallics* **2000**, *19*, 1967–1972. (h) Katayama, H.; Ozawa, F. *Organometallics* **1998**, *17*, 5190–5196. (i) Werner, H.; Lass, R. W.; Gevert, O.; Wolf, J. *Organometallics* **1997**, *16*, 4077–4088. (j) Connelly, N. G.; Geiger, W. E.; Lagunas, M. C.; Metz, B.; Rieger, A. L.; Rieger, P. H.; Shaw, N. J. *J. Am. Chem. Soc.* **1995**, *117*, 12202–12208. (k) Werner, H.; Baum, M.; Schneider, D.; Windmüller, B. *Organometallics* **1994**, *13*, 1089–1097.
- (13) (a) Shirakawa, E.; Nakayama, K.; Morita, R.; Tschimoto, T.; Kawakami, Y.; Matsubara, T. *Bull. Chem. Soc. Jpn.* **2006**, *79*, 1963–1976. (b) Venkatesan, K.; Fox, T.; Schmalke, H. W.; Berke, H. *Eur. J. Inorg. Chem.* **2005**, 901–909. (c) Venkatesan, K.; Blaque, O.; Fox, T.; Schmalke, H. W.; Kheradmandan, S.; Berke, H. *Organometallics* **2005**, *24*, 920–932. (d) Venkatesan, K.; Fox, T.; Schmalke, H. W.; Berke, H. *Organometallics* **2004**, *23*, 1183–1186. (e) Baum, M.; Mahr, N.; Werner, H. *Chem. Ber.* **1994**, *127*, 1877–1886.

- (14) (a) Soriano, E.; Marco-Constelles, J. *Organometallics* **2006**, *25*, 4542–4553. (b) Lin, M.-Y.; Maddirala, S. J.; Liu, R.-S. *Org. Lett.* **2005**, *7*, 1745–1748. (c) Mamane, V.; Hannen, P.; Fürstner, A. *Chem.—Eur. J.* **2004**, *10*, 4556–4575. (d) Miura, T.; Iwasawa, N. *J. Am. Chem. Soc.* **2002**, *124*, 518–519.
- (15) (a) Millert, D. C.; Angelici, R. J. *Organometallics* **1991**, *10*, 79–89. (b) Millert, D. C.; Angelici, R. J. *Organometallics* **1991**, *10*, 99–91.
- (16) (a) Singh, V. K.; Bustelo, E.; De los Ríos, I.; Macías-Arce, I.; Puerta, M. C.; Valerga, P.; Ortuño, M. A.; Ujaque, G.; Lledós, A. *Organometallics* **2011**, *30*, 4014–4031. (b) De los Ríos, I.; Bustelo, E.; Puerta, M. C.; Valerga, P. *Organometallics* **2010**, *29*, 1740–1749.
- (17) Shaw, M. J.; Bryant, S. W.; Rath, N. *Eur. J. Inorg. Chem.* **2007**, 3943–3946.
- (18) (a) Mutoh, Y.; Kimura, Y.; Ikeda, Y.; Tsuchida, N.; Takano, K.; Ishii, Y. *Organometallics* **2012**, *31*, 5151–5158. (b) Mutoh, Y.; Imai, K.; Kimura, Y.; Ikeda, Y.; Ishii, Y. *Organometallics* **2011**, *30*, 204–207. (c) Ikeda, Y.; Yamaguchi, T.; Kanao, K.; Kimura, K.; Kamimura, S.; Mutoh, Y.; Tanabe, Y.; Ishii, Y. *J. Am. Chem. Soc.* **2008**, *130*, 16856–16857.
- (19) Otsuka, M.; Tsuchida, N.; Ikeda, Y.; Kimura, Y.; Mutoh, Y.; Ishii, Y.; Takano, K. *J. Am. Chem. Soc.* **2012**, *134*, 17746–17756.
- (20) (a) Becker, E.; Stingl, V.; Dazinger, G.; Mereiter, K.; Kirchner, K. *Organometallics* **2007**, *26*, 1531–1535. (b) Becker, E.; Stingl, V.; Dazinger, G.; Puchberger, M.; Mereiter, K.; Kirchner, K. *J. Am. Chem. Soc.* **2006**, *128*, 6572–6573.
- (21) Fantasia, S.; Jacobsen, H.; Luigi, C.; Nolan, S. P. *Organometallics* **2007**, *26*, 3286–3288.
- (22) (a) Cabeza, J. A.; Pérez-Carreño, E. *Organometallics* **2010**, *29*, 3973–3978. (b) Vastine, B. A.; Hall, M. B. *Organometallics* **2008**, *27*, 4325–4333. (c) Bassetti, M.; Cadierno, V.; Gimeno, J.; Pasquini, C. *Organometallics* **2008**, *27*, 5009–50016. (d) Zhu, J.; Lin, Z. In *Metal Vinylidenes and Allenylidenes in Catalysis*; Bruneau, C., Dixneuf, P. H., Eds.; Wiley-VCH: Weinheim, Germany, 2008; pp 129–157. (e) Grotjahn, D. B.; Zeng, X.; Cooksy, A. L.; Kassel, W. S.; DiPasquale, A. G.; Sakharov, L. N.; Rheingold, A. L. *Organometallics* **2007**, *26*, 3385–3402. (f) De Angelis, F.; Sgamellotti, A.; Re, N. *Organometallics* **2007**, *26*, 5285–5288. (g) Grotjahn, D. B.; Zeng, X.; Cooksy, A. L. *J. Am. Chem. Soc.* **2006**, *128*, 2798–2799. (h) de Angelis, F.; Sgamellotti, A.; Re, N. *Dalton Trans.* **2004**, 3225–3230. (i) Wakatsuki, Y. *J. Organomet. Chem.* **2004**, *689*, 4092–4109. (j) García-Yebra, C.; López-Mardomingo, C.; Fajardo, M.; Antiñolo, A.; Otero, A.; Rodríguez, A.; Vallat, A.; Luca, D.; Mugnier, Y.; Carbó, J. J.; Lledós, A.; Bo, C. *Organometallics* **2000**, *19*, 1749–1765.
- (23) Bahr, S. R.; Boudjouk, P. *J. Org. Chem.* **1992**, *57*, 5545–5547.
- (24) Štěpánka, J.; Dračinský, M.; Císařová, I.; Kotora, M. *Eur. J. Org. Chem.* **2008**, 47–51.
- (25) Sheldrick, G. M. *SADABS*; University of Göttingen: Göttingen, Germany, 2001.
- (26) (a) Sheldrick, G. M. *SHELXTL, version 6.10, Crystal Structure Analysis Package*; Bruker AXS: Madison, WI, 2000. (b) Sheldrick, G. M. *Acta Crystallogr.* **2008**, *A64*, 112–122.
- (27) Farrugia, L. J. ORTEP-3 for Windows, version 1.076. *J. Appl. Crystallogr.* **1997**, *30*, S65.